# DETERMINATION OF ENERGETIC CHARACTERISTICS OF URBAN-RURAL SURFACES IN THE GREATER ST. LOUIS AREA*

WALTER F. DABBERDT and PAUL A. DAVIS
*Stanford Research Institute, Menlo Park, Calif., U.S.A.*

(Received in final form 29 June, 1977)

**Abstract.** The role of surface geographical characteristics (e.g., albedo, thermal admittance, Bowen ratio, roughness) in the partitioning of energy at the complex and heterogeneous surface of several urban and rural land-use types has been evaluated through an application of Lettau's climatonomy theory. In contrast to the more conventional approach that first specifies all appropriate surface descriptors and then uses them to define climatic features, this application of climatonomy permits the determination of select surface descriptors on the basis of the observed diurnal response of surface temperature to the observed forcing function of available solar energy. Analyses were conducted for a variety of land-use types: urban residential, urban commercial, suburban, and rural farmlands and woods.

The solar forcing function and primary response function (i.e., effective surface temperature) were measured from repetitive diurnal aircraft flights over the greater St. Louis area during clear skies in August 1972. An estimate of surface roughness and subsequent parameterization of the atmospheric sensible heat flux were required for the analyses over nine selected sites. Photosynthetic and anthropogenic fluxes were not considered explicitly. The derived effective thermal admittance (square root of product of heat capacity and thermal conductivity) ranged from a minimum near 20 mly $s^{-1/2}$ $K^{-1}$ for urban and suburban sites to about 85 for wooded sections. The derived inverse Bowen ratio (ratio of latent to sensible heat fluxes) ranged from about 0.22 in the urban area to 2.9 for farmland.

## 1. Introduction

The complex air–earth interface plays an important role in the structure of the atmospheric planetary boundary layer and in the determination of rural and urban climatic differences. Understanding these differences is complicated by the local heterogeneity of individual surface types (i.e., land-use patterns) and the attendant difficulties in parameterization of the interface energy fluxes. Conventional approaches to this problem implicitly consider local areas to be homogeneous on a broad scale and proceed first to specify the appropriate surface geophysical descriptors (e.g., albedo, thermal admittance, roughness) and subsequently to compute the energy fluxes. One of the major difficulties in this approach is the *a priori* specification of surface descriptors. To overcome this limitation, we have evaluated a method by which these descriptors are determined through an examination of variations of the surface energy budget as a function of land use (ranging from rural farmlands to suburbia to the urban fringe). Accordingly, one major objective of this study was to examine the feasibility of obtaining representative empirical data depicting the

* Research sponsored by the Environmental Protection Agency under Contract No. 68-02-1015.

*Boundary-Layer Meteorology* **14** (1978) 105–121. 

influence of the surfaces on the establishment of rural-urban differences in the surface energy budget.

In the climatonic approach (Lettau and Lettau, 1972), temporal climatic variations are described analytically as unique response functions to a prescribed forcing function. More specifically, climatonomy may be summarized as the quantitative determination of mean values and temporal-spatial variations of: temperature, the primary response function; and energy fluxes, the secondary responses (e.g., atmospheric and subsurface sensible heat exchanges, net effective infrared emissions, evaporation) at a planetary surface in response to the solar forcing function (i.e., available incident solar radiation).

The experimental program focused first on acquisition of data on the spatial and temporal (i.e., diurnal) distribution of surface temperature and on solar and terrestrial radiation for a variety of surfaces. Data sources comprised: (1) frequent aircraft observations; (2) continuous surface observations; and (3) supplemental, conventional observations. The aircraft observations* consisted of flights at two- and three-hourly intervals over a 90-km path centered over the St. Louis urban core; to obtain as much independent data as possible, the initial and return legs of each flight were made at different altitudes. The primary aircraft data included both upwelling and downwelling solar irradiance and effective surface radiative temperature. Supplemental aircraft observations included surface photography and ambient temperature. Representative measurements of the albedo (based on upwelling irradiance measurements) and surface temperature (based on upwelling radiance measurements) are difficult to acquire except from a moving platform aloft.

At this stage of investigation, a study of direct influences of the atmospheric boundary layer itself on the radiative processes was not emphasized. Instead, representative measurements of total downwelling irradiance were made at one surface site to incorporate any atmospheric influence directly. The other principal data requirement is the boundary-layer wind profile; this was available twice daily from the Environmental Meteorological Support Unit (EMSU) station located in downtown St. Louis and operated by the National Weather Service (NWS).

Surface geophysical features derived through the analysis of the surface response to the radiative forcing function were limited to two parameters: thermal admittance and inverse Bowen ratio. This limitation was a result of the number and type of measured values; to derive additional geophysical features would have required additional measurements, such as the latent or sensible heat fluxes. Even so, certain simplifying assumptions had to be made. Photosynthetic and anthropogenic fluxes of heat were not treated explicitly in the theory; however, their actual impacts on the observations are implicit in the data and thus are reflected in the derived values. Moreover, the August data used in the analysis have the advantage that the absolute contributions from both processes to the surface energy balance are for the most part minimal, although finite for certain land-use types considered.

* Provided by the Colorado State University, Fort Collins, Colorado, under subcontract to SRI.

## 2. Climatonomy Theory

Lettau* coined the term climatonomy in 1954 to emphasize quantitative aspects of the subject; thus climatonomy denotes the use of numerical models to solve the local surface energy budget equation. Surface energy budget theory expresses the principle of the conservation of energy in the partitioning of the effective incoming solar radiation at the earth–air interface. For the case of local homogeneity, the surface energy budget is given by

$$F_0 = LW_0\uparrow - LW_0\downarrow + S_0 + Q_0 + E_0 + P_0 , \tag{1}$$

where

$F_0 \equiv$ solar forcing function (cal cm$^{-2}$ s$^{-1}$); the effective short-wave radiation at the surface,
$LW_0\uparrow \equiv$ upwelling long-wave radiation at the surface,
$LW_0\downarrow \equiv$ downwelling long-wave radiation at the surface,
$S_0 \equiv$ subsurface heat flux density,
$Q_0 \equiv$ atmospheric heat flux density,
$E_0 \equiv$ evaporative heat flux density,
$P_0 \equiv$ photosynthetic heat flux density.

By definition, heat flux away from the surface is defined as positive. For the urban surface, photosynthetic energy transforms can usually be ignored; however, on the overall average, they may account for 5 to 10% of the available solar energy (Van Wijk, 1963). Although further work should evaluate this impact of vegetation on rural-urban climatic differences, we ignored this term in this exploratory study.

In climatonomy, the energy budget is examined over basic meteorological periods (e.g., diurnal and annual) through the use of 'Fourier synthesis'. Thus each term in Equation (1) is represented by a mean value and harmonics. Expanding each term in Equation (1) we obtain

$$F_0 = \bar{F}_0 + \sum_{i=1}^{m} \Delta_i F_0 \cos(\text{int} - \delta_i) , \tag{2a}$$

$$LW_0\uparrow = \overline{LW_0\uparrow} + \sum_{i=1}^{m} \Delta_i LW_0\uparrow \cos(\text{int} - \delta_i + \gamma_i^*) , \tag{2b}$$

$$LW_0\downarrow = \overline{LW_0\downarrow} + \sum_{i=1}^{m} \Delta_i LW_0\downarrow \cos(\text{int} - \delta_i + \beta_i^*) , \tag{2c}$$

$$S_0 = \overline{S_0} + \sum_{i=1}^{m} \Delta_i S_0 \cos(\text{int} - \delta_i + \psi_i^*) , \tag{2d}$$

$$Q_0 = \overline{Q_0} + \sum_{i=1}^{m} \Delta_i Q_0 \cos(\text{int} - \delta_i + \varphi_i^*) , \tag{2e}$$

* Annual meeting of the American Geophysical Union, Washington, D.C. (1954).

$$E_0 = \overline{E_0} + \sum_{i=1}^{m} \Delta_i E_0 \cos(\text{int} - \delta_i + \chi_i^*), \tag{2f}$$

where $t$ is time, $i$ is the harmonic order, $n$ is the basic frequency when $n = 2\pi/\tau$ and $\tau$ is the basic period (i.e., one day). In Equation (2), $\Delta_i(\ )$ is the amplitude of the $i$th harmonic, $\delta_i$ is the phase angle for the $i$th harmonic of the forcing function, and $(\ )_i^*$ is the phase lag of the various response functions to the solar phase. In the analyses that follow, zero time reference corresponds to midnight. The overbar denotes the time-averaged value over the basic period.

A basic premise of climatonomy is that the primary response to the solar forcing function is the surface temperature and that the 'climatic' functions are secondary responses, via the surface temperature, to the solar forcing function. In other words, each of the climatic functions can be expressed in terms of surface temperature; hence, Equations (1) can be solved to yield a unique set of mean values plus variations of the response terms. Thus, it is appropriate to introduce first the Fourier representation for the surface temperature and then to rewrite the secondary response functions in terms of surface temperature, where

$$T_0 = \overline{T_0} + \sum_{i=1}^{m} \Delta_i T_0 \cos(\text{int} - \delta_i^*) \tag{3a}$$

and

$$T_0 = \overline{T_0} + \sum_{i=1}^{m} (\Delta_i F_0 / Z_i) \cos(\text{int} - \delta_i - \zeta_i), \tag{3b}$$

where

$$Z_i \equiv \Delta_i F_0 / \Delta_i T_0, \tag{4a}$$

and

$$\zeta_i \equiv \delta_i^* - \delta_i. \tag{4b}$$

Furthermore,

$$LW_0\uparrow = \overline{LW_0\uparrow} + \sum_{i=1}^{m} (\Gamma_i \Delta_i T_0) \cos(\text{int} - \delta_i - \zeta_i + \gamma_i), \tag{5a}$$

$$LW_0\downarrow = \overline{LW_0\downarrow} + \sum_{i=1}^{m} (B_i \Delta_i T_0) \cos(\text{int} - \delta_i - \zeta_i + \beta_i), \tag{5b}$$

$$S_0 = \overline{S_0} + \sum_{i=1}^{m} (\Psi_i \Delta_i T_0) \cos(\text{int} - \delta_i - \zeta_i + \psi_i), \tag{5c}$$

$$Q_0 = \overline{Q_0} + \sum_{i=1}^{m} (\Phi_i \Delta_i T_0) \cos(\text{int} - \delta_i - \zeta_i + \varphi_i), \tag{5d}$$

$$E_0 = \overline{E_0} + \sum_{i=1}^{m} (X_i \Delta_i T_0) \cos(\text{int} - \delta_i - \zeta_i + \chi_i), \tag{5e}$$

where the following identities are introduced

$$\Delta_i L W_0\uparrow \equiv \Gamma_i \Delta_i T_0\,, \qquad \gamma_i^* \equiv -\zeta_i + \gamma_i\,; \tag{6a}$$

$$\Delta_i L W_0\downarrow \equiv B_i \Delta_i T_0\,, \qquad \beta_i^* \equiv -\zeta_i + \beta_i\,; \tag{6b}$$

$$\Delta_i S_0 \equiv \Psi_i \Delta_i T_0\,, \qquad \psi_i^* \equiv -\zeta_i + \psi_i\,; \tag{6c}$$

$$\Delta_i Q_0 \equiv \Phi_i \Delta_i T_0\,, \qquad \varphi_i^* \equiv -\zeta_i + \varphi_i\,; \tag{6d}$$

$$\Delta_i E_0 \equiv X_i \Delta_i T_0\,, \qquad \chi_i^* \equiv -\zeta_i + \chi_i\,. \tag{6e}$$

When the identity (4a) is introduced, Equations (2a) is rewritten as

$$F_0 = \overline{F_0} + \sum_{i=1}^{m} (Z_i \Delta_i T_0) \cos(\text{int} - \delta_i)\,. \tag{7}$$

Lettau then introduces Equations (5) and (7) into (1), and expands the cosine functions. The basic cycle average equation is subtracted, leaving only a departure equation that is evaluated at $\text{int} = \delta_i$ and $\text{int} = \delta_i + \pi/2$ to yield two simultaneous, independent equations, where:

$$\tan \zeta_i = \frac{-B_i \sin \beta_i + \Gamma_i \sin \gamma_i + \Psi i \sin\ \psi_i + \Phi_i \sin \phi_i + X_i \sin \chi_i}{-B_i \cos \beta_i + \Gamma_i \cos \gamma_i + \Psi_i \cos\ \psi_i + \Phi_i \cos \phi_i + \chi_i \cos \chi_i} \tag{8}$$

and

$$Z_i = -B_i \cos(\zeta_i - \beta_i) + \Gamma_i \cos(\zeta_i - \gamma_i) + \Psi_i \cos(\zeta_i - \psi_i) + \Phi_i \cos(\zeta_i - \varphi_i) + X_i \cos(\zeta_i - \chi_i)\,. \tag{9}$$

Not all of the amplitude and phase terms are obtainable directly from the St. Louis observations. Hence, we need to consider the parameterization of these terms on the basis of identifiable surface features.

Parameterization of the upwelling infrared flux at the surface is straightforward through application of the Stefan–Boltzmann law,

$$L W_0\uparrow = \varepsilon \sigma T_0^4\,, \tag{10}$$

where $\varepsilon$ is the surface emissivity and $\sigma$ is the universal Stefan–Boltzmann constant ($0.813 \times 10^{-7}$ mly min$^{-1}$ K$^{-4}$). Introducing Equation (10) into Equation (3a) and solving for the partial impedance and phase, we obtain

$$\Gamma_i \simeq 4\overline{L W_0\uparrow}/\overline{T_0}\,, \tag{11a}$$

and

$$\gamma_i = 0\,. \tag{11b}$$

The partial impedance $B_i$ and phase $\beta_i$ for the downwelling long-wave flux at the surface have not been parameterized here. Instead, they were obtained through Fourier analysis of the continuous diurnal pyrgeometer measurements made at the ground station.

The subsurface heat flux density is parameterized through the application of Fourier's law of heat conduction (Equation (12a)) and the continuity equation for heat in the absence of sources and sinks (Equation (12b)), where

$$S = -\lambda \frac{\partial T}{\partial z} \tag{12a}$$

and

$$\frac{\partial S}{\partial z} = -C \frac{\partial T}{\partial t} \tag{12b}$$

Here $\lambda$ is the thermal conductivity (cal $cm^{-1}$ $K^{-1}$ $min^{-1}$) and $C$ is the volumetric heat capacity (cal $K^{-1}$ $cm^{-3}$) of the submedium. If the medium is considered as an equivalent homogeneous conductor ($\partial\lambda/\partial z = \partial C/\partial z = 0$) with time-independent thermal coefficients ($\partial\lambda/\partial t = \partial C/\partial t = 0$), the partial impedance $\Psi_i$ and phase $\psi_i$ are given as

$$\Psi_i = (\lambda C \text{ in})^{1/2} \equiv \mu (\text{in})^{1/2}, \tag{12c}$$

and

$$\psi_i = \pi/4, \tag{12d}$$

where $\mu$ (cal $K^{-1}$ $cm^{-2}$ $min^{-1/2}$) is defined as the thermal admittance.

Parameterization of the atmospheric heat flux density is perhaps the most difficult. Lettau and Lettau (1972) present a type of similarity approach based on the near-surface vertical profile of potential temperature. Both the partial impedance $\Phi_i$ and the phase $\varphi_i$ are given in terms of a characteristic number $N_i$ that is a unique function of the frequency, aerodynamic surface roughness $z_0$, and the mean friction velocity $\overline{V^*}$, where

$$N_i = \log_{10}\left(\frac{\overline{V^*}}{in\, z_0}\right). \tag{13}$$

The partial impedance $\Phi_i$ is then expressed as

$$\Phi_i = \frac{\rho C_p \overline{V^*}}{(a + bN_i)(1 - M^*)}. \tag{14a}$$

The term $M^*$ expresses the magnitude of convective mixing relative to mechanical turbulence; its absolute value is proportional to $\overline{Q_0}/\overline{V^*}$ and is less than unity, and its sign is determined by that of $\overline{Q_0}$. For urban areas, $\overline{V^*}$ will usually be large because of the tall roughness elements; hence, $M^*$ will be small. When buoyancy effects on turbulent diffusion of heat are assumed to be small in comparison with mechanical mixing, diurnal variations of $M^*$ are similarly small $[(\tau/_i M^*)\, \partial M^*/\partial t \simeq 0]$ and Equation (14a) can be simplified accordingly, where

$$\Phi_i \approx \frac{\rho C_p \overline{V^*}}{(a + bN_i)(1 - \overline{M^*})}. \tag{14b}$$

Lettau also gives an expression for the phase lag,

$$\varphi_i = \tan^{-1}\left(\frac{c}{a+bN_i}\right), \tag{14c}$$

where $a$, $b$, and $c$ are semi-empirical constants.

It would have been impractical, if not impossible, to determine $V^*$ and $z_0$ directly along the flight path; consequently, these also had to be estimated. Values for $z_0$ were derived from an empirical relationship developed by Kung (1963),

$$\log_{10} z_0 = -1.24 + 1.19 \log h^*, \tag{15a}$$

where $h^*$ is the characteristic physical height of the roughness elements. The term $V^*$ is, in turn, also derived from an empirical equation from Kung based on the relationship between the geostrophic drag coefficient $C_D$ and the surface Rossby number Ro,

$$C_D \equiv V^*/V_g = 0.174/(\log_{10} \mathrm{Ro} - 0.81) \tag{15b}$$

$$\mathrm{Ro} \equiv V_g/z_0 f, \tag{15c}$$

where $V_g$ is the geostrophic wind and $f$ the Coriolis parameter.

In this study a simplistic approach toward the parameterization of evaporation has been taken with $E_0$ expressed in terms of $Q_0$ by using the inverse Bowen ratio Bo. Thus,

$$X_i = \mathrm{Bo}\, \Phi_i, \tag{16a}$$

and

$$\chi_i = \varphi_i. \tag{16b}$$

In the following section the reduction of the observations is discussed in terms of the input requirements of the theory as well as its application for the evaluation of the evaporative and thermal properties of the surface throughout the region.

## 3. Method of Approach

Aircraft observatios were made continuously from each of the two altitudes along the 90-km flight path (Figure 1); portions of the flight track corresponding to distinctly different (yet individually homogeneous) surface types were isolated and average meteorological conditions representative of each type were obtained. Table I describes nine surface sites selected for analysis. Rural sites on opposite sides of the urban core were chosen so as to examine possible skewness in the climatic distribution that might arise from advection associated with the urban heat island. The sites were carefully evaluated to ensure reasonable homogeneity over a scale of several kilometres and to minimize the impact of discontinuities in land use. Digitized records of the hemispheric solar radiation measurements from the aircraft were

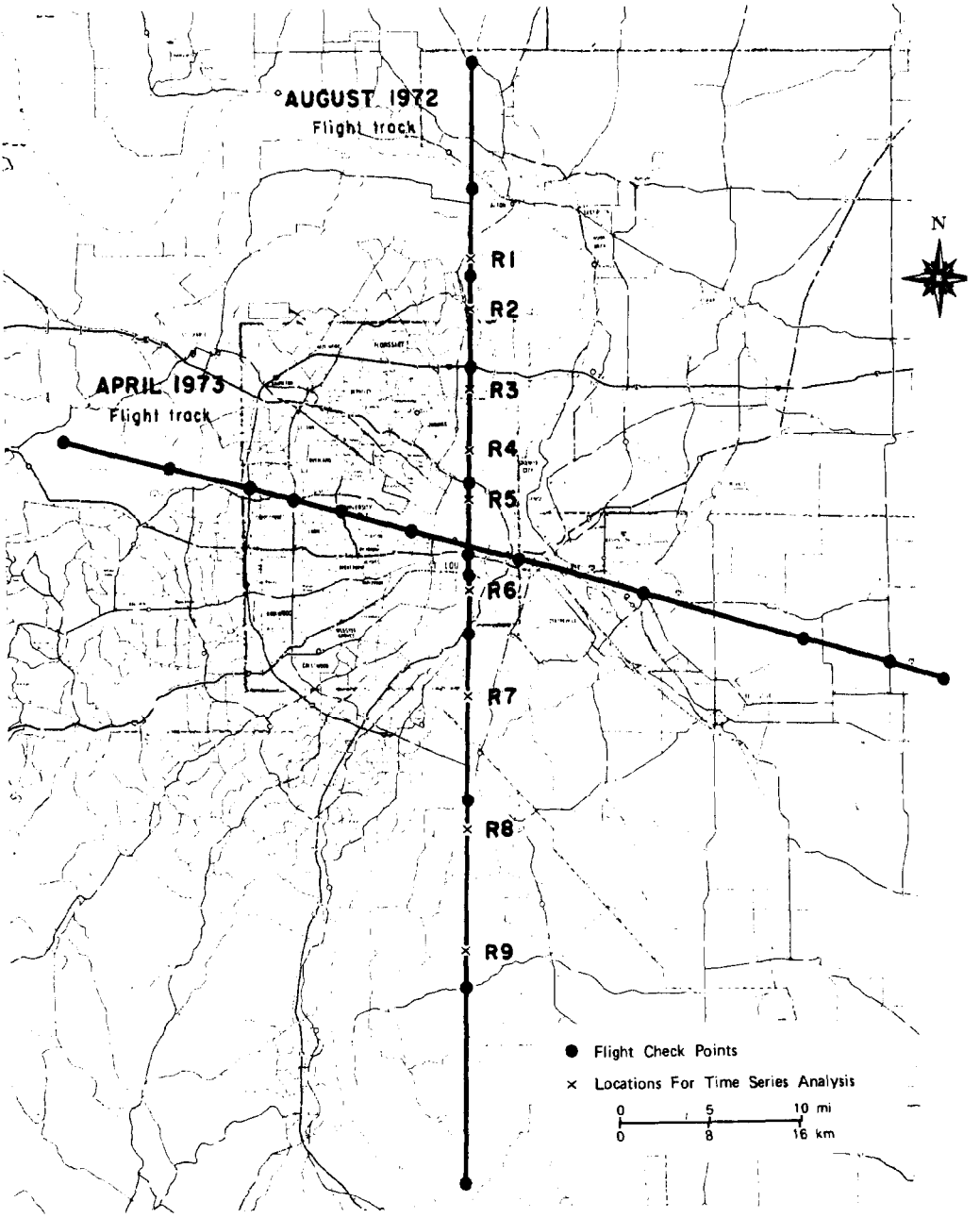


Fig. 1. Flight tracks, check points, and locations selected for harmonic analysis of data.

TABLE I

Surface areas selected for analysis

| Site[a] | Description | Range (km)[b] |
|---|---|---|
| R-1 | Mostly farmland; roadway; some trees | 23.8 N |
| R-2 | Mostly woods, some fields; roadways | 19.9 N |
| R-3 | New suburban housing tract | 13.0 N |
| R-4 | Commercial–industrial; old residential | 7.8 N |
| R-5 | Old urban residential | 3.7 N |
| R-6 | Old urban residential; some light commercial | 3.7 S |
| R-7 | Farmland | 12.5 S |
| R-8 | Mostly woods and fields; some farmland | 23.8 S |
| R-9 | Mostly woods, some fields | 33.7 S |

[a] Locations shown in Figure 1.
[b] Distance (north or south) of city centre.

averaged over 15-s periods while 5-s averages were obtained for the higher-resolution infrared radiometer measurements of surface temperature. Summaries of these data over the various sites were used in the analysis of the surface energy budget.

The reduction of the surface observations of downwelling long-wave and solar radiation in terms of the requirements of the theory (Equations (2a) and (2c)) is straightforward and entails only the direct application of harmonic analysis (see, for example, Panofsky and Brier, 1965). Recalling Equation (2a) and expressing the absorbed solar radiation at the surface (i.e., the surface forcing function) in terms of the insolation $F_0\downarrow$ and the surface albedo $a$, we obtain

$$F_0 = F_0\downarrow - F_0\uparrow = F_0\downarrow(1-a)$$

$$= (1-a)\left[\overline{F_0\downarrow} + \sum_{i=1}^{m} \Delta_i F_0\downarrow \cos(\text{int} - \delta_i)\right], \tag{17}$$

when the albedo is time-independent. Because the 9 August measurements entail solar data on only the five daytime flights, well above the surface, these aircraft observations were used to determine only the mean albedo of each of the nine representative surface types.

The insolation measured at the surface station is used in the evaluation of Equation (17) under the assumption that spatial variations of $F_0\downarrow$ along the flight track were negligible on this day. Values at 30-min intervals were taken from the analog trace, and the amplitude and phase terms were computed for 24 harmonics; the results are summarized later (in Table III). Only the first and second harmonics are listed because they account for 98.8% of the total variance.

The downwelling infrared flux density as recorded at the surface station was also assumed representative of conditions at each of the nine sites. As above, the harmonic analysis of values at 30-min intervals were performed in the evaluation of

Equation (2c). In general agreement with the solar data, 95.6% of the variance is specified by the first and second harmonics.

Determination of a daily average and the harmonics for the aircraft observations cannot be obtained through standard harmonic analysis due to the irregular temporal spacing of the seven averaged data points representative of each surface region as measured at each of the two altitudes. Furthermore, the small number of data points and relatively large time intervals prevented the use of extrapolation methods. Hence, we evaluated the applicability of a nonlinear regression routine available at SRI. In this manner, we specified the form of the Fourier series and obtained the mean, amplitude, and phase that best fit the data. A two-harmonic function was chosen, resulting in a five-parameter fit to the data:

$$T(t) = R_1 + R_2 \cos(0.2618t - R_3) + R_4 \cos(0.5236t - R_5), \tag{18}$$

where

$R_1$ = period average (°C),
$R_2$ = amplitude of 1st harmonic (°C),
$R_3$ = phase of 1st harmonic (rad),
$R_4$ = amplitude of 2nd harmonic (°C),
$R_5$ = phase of 2nd harmonic (rad).

The form of the equation is directly analogous to that of Equations (2a) through (2f). Before the technique was applied to the reduction of the aircraft data, the method was first evaluated by testing it on near-surface thermographic data obtained from seven instrument shelters maintained throughout the area by the Illinois State Water Survey (ISWS) (Changnon, 1972). After these strip chart data were reduced to provide 24-hourly temperature values at each station, they were analyzed with both the conventional harmonic analysis method for all 24 values and the regression method with only eight values. Data points were chosen at times corresponding to the times of the seven aircraft flights plus an additional value at midnight. Results obtained from the regression method for all seven stations are in excellent agreement with those of the harmonic analysis for both the mean values and the first harmonics while the second harmonic values agreed quite satisfactorily.

The regression method was applied to the analysis of the effective surface temperature data obtained from the aircraft measurements. The nighttime portions of the fitted curves were unrepresentative compared with the shape of the near-surface ambient temperature curves for the seven ISWS stations. This discrepancy resulted from the large time interval between the last evening datum and the first morning value. The importance of one or more measurements during this period was recognized, but we were unable to obtain the additional measurements due to mechanical failure of the aircraft. In lieu of an intermediate measurement, we estimated a reasonable value in order to inhibit dominance of the nighttime regime by the second harmonic. The interpolation is necessarily subjective, although consistent among sites: a value is obtained midway between the 2000 and 0400 CDT (Central Daylight Time) measurements by assuming that 60% of the surface cooling

occurs during the first half of the interval. This rate reflects nighttime surface cooling typical of cloud-free conditions as experienced during the experimental period. The temperature change over this interval was of the order of 10 °C at the nine sites. The magnitude of the uncertainty of the interpolated value is believed to be of the order of 1 °C. The corresponding impacts of a 1 °C error are: $\bar{T} = 0.20$ °C; $\Delta_1 T = -0.22$ °C; $\Delta_2 T = 0.26$ °C; $\delta_1^* = 0.03$ rad; and $\delta_2^* = -0.04$ rad. In view of the relatively small impact of 'errors' as large as 1 °C, we feel confident in the representativeness of the regression analysis using the single interpolated value.

## 4. Application and Results

In view of the available experimental data and the objective of evaluating effective surface geophysical features, the specific aim of the analysis program was to determine the feasibility of obtaining the thermal (i.e., thermal admittance) and evaporative (inverse Bowen ratio) descriptors of a variety of land-use types through the application of climatonomic theory to direct and remote observations. The first step in the analysis is to specify the solar forcing function at each of the sites and then the primary response function (i.e., surface temperature); through parameterization, the secondary responses are specified or evaluated, and then the descriptors are determined.

Table II lists the albedo values observed at each site for all of the daytime flights on 9 August 1972. Summarizing, the summer albedo over the St. Louis urban areas is several percent lower than the albedo over surrounding areas.

TABLE II

Albedo values for nine surface areas, measured on 9 August 1972

| Flight time (approximately) | Site number | | | | | | | | |
|---|---|---|---|---|---|---|---|---|---|
| | R-1 | R-2 | R-3 | R-4 | R-5 | R-6 | R-7 | R-8 | R-9 |
| Altitude: 1220 m | | | | | | | | | |
| 0900 CDT | 16.3 | 16.8 | 16.1 | 13.5 | 11.9 | 12.1 | 14.9 | 16.4 | 16.5 |
| 1130 | 15.9 | 16.6 | 16.8 | 14.0 | 12.5 | 12.9 | 15.0 | 16.2 | 16.6 |
| 1330 | 15.2 | 15.5 | 15.6 | 13.3 | 11.9 | 12.6 | 15.2 | 16.2 | 16.6 |
| 1600 | 15.6 | 15.6 | 16.4 | 14.3 | 13.3 | 15.1 | 17.5 | 19.0 | 16.7 |
| 1900 | 13.8 | 17.9 | 16.1 | 14.2 | 13.1 | 13.4 | 14.4 | 16.6 | 15.4 |
| Average | 15.4 | 16.5 | 16.2 | 13.9 | 12.6 | 13.3 | 15.4 | 16.9 | 16.4 |
| Altitude: 460 m | | | | | | | | | |
| 0900 CDT | 15.9 | 16.2 | 16.3 | 13.8 | 12.0 | 11.9 | 15.1 | 16.2 | 14.9 |
| 1130 | 15.1 | 15.5 | 16.0 | 13.8 | 11.6 | 12.0 | 14.5 | 16.8 | 16.7 |
| 1330 | 14.8 | 17.3 | 16.5 | 13.4 | 12.1 | 12.0 | 14.3 | 16.8 | 16.5 |
| 1600 | 15.7 | 17.3 | 17.4 | 14.3 | 13.1 | 12.5 | 14.9 | 16.3 | 16.6 |
| Average | 15.4 | 16.6 | 16.6 | 13.8 | 12.2 | 12.1 | 14.7 | 16.5 | 16.2 |

Figure 2 illustrates the five-parameter (two-harmonic) fit to the surface temperature data obtained by the aircraft for an urban site and a rural site. The pronounced heat-island effect (greater than 10 °C) at time of maximum surface temperature is apparent. In addition to other differences in response, more solar radiation is absorbed at the urban surface.

Table III lists first the mean, amplitude, and phase terms for the insolation on 9 August. The surface reflectivity determines the form of the forcing function at each site. The diurnal surface temperature variations discussed earlier and illustrated in Figure 2 are the effective surface radiative temperature values deduced from the aircraft measurements and an assumed constant surface emissivity of unity. As discussed earlier, the $B_i$ and $\beta_i$ terms describing the downwelling long-wave flux are derived from the harmonic analysis of the pyrgeometer measurements at the surface station. These values have been taken as representative of conditions at all nine surface test areas.

Estimates of the amplitude and phase terms for the atmospheric flux of sensible heat follow from Equations (13) through (15). The aerodynamic surface roughness is computed with Equation (15a) using characteristic physical heights estimated from the aerial photographs for the various sites. The geostrophic wind was estimated from the two National Weather Service low-level EMSU soundings (0700 and 1230

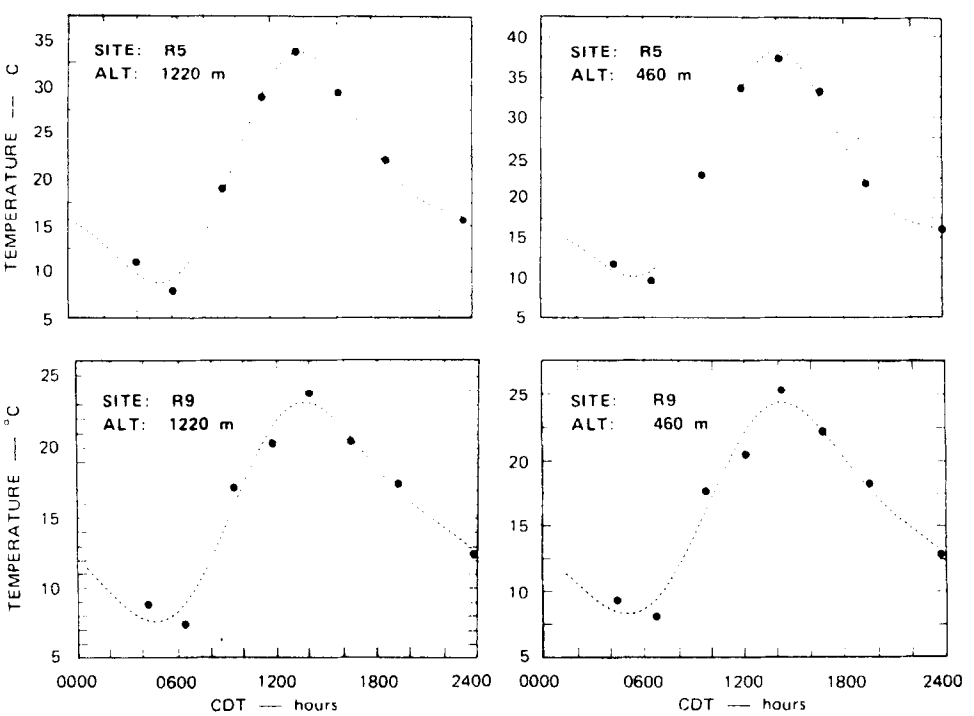


Fig. 2. Effective surface radiative temperature from low aircraft altitudes at two sites on 9 August, 1972. Curve is from 2-harmonic regression analysis.

CDT) to be about 6.5 m $s^{-1}$. After the surface Rossby number at each site was computed, the geostrophic drag coefficient and the surface friction velocity were determined from Equation (15). Terms $\Phi$ and $\varphi$, tabulated in Table III, are based on Equations (14) and the following constant values: $a = b = 8.5$; $c = 17$, and $\bar{M}^* = 0.2$.

Having parameterized the radiative fluxes and the atmospheric sensible heat flux, the solutions for both the evaporative and the subsurface heat fluxes were obtained by using the known amplitude and phase terms together with Equations (8) and (9). Since $\psi$ and $\chi$ are known, both $\Psi$ and $X$ and, subsequently, $\mu$ and Bo can be evaluated with Equations (12c) and (16a), respectively. In the case of the partial impedance for evaporation, the sum of $\Phi$ and $X$ has been evaluated using Equations (8) and (9); the $X$-values are then obtained as the residual by using the $\Phi$-values as discussed above. The thermal admittance $\mu$ follows from $\Psi$ by using Equation (12c). The values for $\Psi$, Bo, and $\mu$ evaluated in this manner by using first-harmonic amplitude and phase terms are summarized in Table III.

## 5. Discussion

In summary, we have taken measured radiative parameters and certain parameterized (synthesized) values and through the application of climatonomy have determined two important geophysical features of the sites: the thermal admittance ($\mu$) is obtained through consideration of the submedium at each site to be a homogeneous conductor of heat; the inverse Bowen ratio (Bo) expresses the magnitude of the evaporative heat flux as a fraction of the atmospheric sensible heat flux at the earth/air interface. Remembering the limitations noted both in the measured and parameterized values, we can subjectively evaluate the representativeness and significance of the results. It is encouraging to note that all sites have $\mu$ and Bo values that are in the range anticipated from conventional measurements at similar, but more uniform and homogeneous, surfaces. For example, $\mu$ ranges from a minimum of 22 mly $s^{-1/2}$ $K^{-1}$ in open farm country (R-7) to a maximum of about 87 at the wooded sites (R-8 and R-9); the mean value for all sites is 42. Geiger (1965) lists typical $\mu$ values determined for a variety of homogeneous media: soils range from 14 mly $s^{-1/2}$ $K^{-1}$ for fine, dry quartz sand to 47 for the same sand with 22% moisture; $\mu$ for 'sandy clay (15% moisture)' is given as 36 while 'swamp land (90% moisture)' is 44. Rocks range from 45 for basalt to 56 for granite and concrete. Regarding heterogeneous surfaces, 'fields, weedy swamp, still water, and hilly woods' have $\mu$ values of 35.

Examining our results in view of this background, we can draw several conclusions. First, the absolute values of the computed thermal admittances are reasonable. Second, the highest values occur at sites R-2, R-8, and R-9. These three sites share one common feature not typical of any of the other six sites: all are dominated by a high percentage of wooded areas. However, it is interesting that Geiger estimates $\mu$ to be smaller by a factor of 1.5 to 2 for similar terrain, although it is uncertain whether his estimate is a summer or winter value. It is conceivable that the presence or

TABLE III

Climatonomic parameters in the greater St. Louis area for 9 August 1972

| Site: altitude | $\bar{F}_0$ (ly min$^{-1}$) | $\Delta_1 F_0$ (ly min$^{-1}$) | $\delta_1$ (rad) | $\Delta_2 F_0$ (ly min$^{-1}$) | $\delta_2$ (rad) | $\bar{T}_0$ (K) | $\Delta_1 T_0$ (K) | $\zeta_1$ (rad) | $\Delta_2 T_0$ (K) | $\zeta_2$ (rad) | $Z_1$ (mly min$^{-1}$ K$^{-1}$) | $Z_2$ | $\Gamma_{1,2}$ (mly min$^{-1}$ K$^{-1}$) | $\gamma_{1,2}$ (rad) | $B_1$ (mly min$^{-1}$ K$^{-1}$) | $\beta_1$ (rad) |
|---|---|---|---|---|---|---|---|---|---|---|---|---|---|---|---|---|
| R1:U | 0.362 | 0.547 | 3.429 | 0.199 | 0.555 | 290.2 | 9.65 | 0.50 | 3.58 | −0.24 | 59.3 | 62.5 | 7.9 | 0 | 6.2 | 0.20 |
| R1:L | 0.362 | 0.547 | 3.429 | 0.199 | 0.555 | 291.8 | 10.44 | 0.50 | 3.62 | 0.07 | 55.4 | 67.4 | 8.1 | 0 | 5.7 | 0.20 |
| R2:U | 0.357 | 0.540 | 3.429 | 0.196 | 0.555 | 289.8 | 7.99 | 0.59 | 2.61 | −0.22 | 67.0 | 72.1 | 7.9 | 0 | 7.5 | 0.29 |
| R2:L | 0.357 | 0.540 | 3.429 | 0.196 | 0.555 | 291.3 | 9.23 | 0.48 | 3.62 | 0.14 | 57.2 | 48.7 | 8.1 | 0 | 6.5 | 0.18 |
| R3:U | 0.358 | 0.542 | 3.429 | 0.197 | 0.555 | 289.8 | 8.26 | 0.43 | 3.34 | −0.04 | 65.2 | 65.2 | 7.9 | 0 | 7.3 | 0.13 |
| R3:L | 0.357 | 0.540 | 3.429 | 0.196 | 0.555 | 291.3 | 8.76 | 0.46 | 3.34 | 0.04 | 62.9 | 57.1 | 8.0 | 0 | 6.8 | 0.16 |
| R4:U | 0.369 | 0.557 | 3.429 | 0.203 | 0.555 | 291.0 | 9.00 | 0.51 | 4.19 | 0.21 | 61.9 | 47.6 | 8.0 | 0 | 6.7 | 0.21 |
| R4:L | 0.369 | 0.557 | 3.429 | 0.203 | 0.555 | 294.5 | 12.26 | 0.48 | 4.96 | 0.47 | 44.2 | 39.1 | 8.3 | 0 | 4.9 | 0.18 |
| R5:U | 0.374 | 0.565 | 3.429 | 0.205 | 0.555 | 293.0 | 10.65 | 0.51 | 3.80 | 0.05 | 52.7 | 54.0 | 8.2 | 0 | 5.6 | 0.21 |
| R5:L | 0.376 | 0.568 | 3.429 | 0.206 | 0.555 | 294.9 | 12.33 | 0.48 | 4.49 | 0.29 | 45.9 | 44.9 | 8.3 | 0 | 4.9 | 0.18 |
| R6:U | 0.371 | 0.561 | 3.429 | 0.204 | 0.555 | 293.2 | 10.40 | 0.47 | 3.78 | −0.00 | 52.7 | 49.8 | 8.2 | 0 | 5.8 | 0.17 |
| R6:L | 0.376 | 0.568 | 3.429 | 0.206 | 0.555 | 295.6 | 11.88 | 0.45 | 4.46 | 0.12 | 44.4 | 38.7 | 8.4 | 0 | 5.1 | 0.15 |
| R7:U | 0.362 | 0.547 | 3.429 | 0.199 | 0.555 | 289.8 | 8.68 | 0.44 | 3.26 | −0.42 | 61.5 | 57.4 | 7.9 | 0 | 6.8 | 0.14 |
| R7:L | 0.365 | 0.552 | 3.429 | 0.200 | 0.555 | 292.2 | 10.69 | 0.38 | 3.42 | −0.23 | 51.4 | 58.4 | 8.1 | 0 | 5.6 | 0.08 |
| R8:U | 0.356 | 0.538 | 3.429 | 0.196 | 0.555 | 288.3 | 6.90 | 0.67 | 1.52 | −0.75 | 80.3 | 113.5 | 7.8 | 0 | 8.7 | 0.37 |
| R8:L | 0.357 | 0.540 | 3.429 | 0.196 | 0.555 | 288.9 | 7.67 | 0.51 | 2.10 | −0.57 | 71.9 | 99.6 | 7.8 | 0 | 7.8 | 0.21 |
| R9:U | 0.358 | 0.542 | 3.429 | 0.197 | 0.555 | 288.5 | 7.00 | 0.52 | 1.80 | −0.39 | 76.5 | 96.8 | 7.8 | 0 | 8.6 | 0.22 |
| R9:L | 0.358 | 0.542 | 3.429 | 0.197 | 0.555 | 289.1 | 7.38 | 0.57 | 1.72 | −0.14 | 74.1 | 125.4 | 7.9 | 0 | 8.1 | 0.27 |

*Table III (continued)*

| Site: altitude | $B_2$ (mly min$^{-1}$ K$^{-1}$) | $\beta_2$ (rad) | $z_0$ (cm) | $V^*$ (cm s$^{-1}$) | $\Phi_1$ (mly min$^{-1}$ K$^{-1}$) | $\varphi_1 = \chi_1$ (rad) | $\Phi_2$ (mly min$^{-1}$ K$^{-1}$) | $\varphi_2 = \gamma_2$ (rad) | $\psi_{1,2}$ rad | $\Psi_1$ (mly min$^{-1}$ K$^{-1}$) | $\Psi_2$ | $\mu$ (mly s$^{-1/2}$ K$^{-1}$) | $B_0$ (n.d.) |
|---|---|---|---|---|---|---|---|---|---|---|---|---|---|
| R1:U | 5.3 | −0.65 | 15 | 23 | 10.7 | 0.36 | 11.4 | 0.38 | 0.79 | 23.7 | −86.0 | 46 | 2.10 |
| R1:L | 5.2 | −0.34 | 15 | 23 | 10.7 | 0.36 | 11.4 | 0.38 | 0.79 | 22.5 | −44.0 | 44 | 1.74 |
| R2:U | 7.3 | −0.63 | 50 | 26 | 13.2 | 0.39 | 14.1 | 0.41 | 0.79 | 40.7 | −132.0 | 80 | 1.18 |
| R2:L | 5.2 | −0.27 | 50 | 26 | 13.2 | 0.39 | 14.1 | 0.41 | 0.79 | 18.0 | −41.3 | 35 | 2.06 |
| R3:U | 5.7 | −0.45 | 100 | 28 | 15.0 | 0.41 | 16.1 | 0.44 | 0.79 | 6.6 | −83.1 | 13 | 2.94 |
| R3:L | 5.7 | −0.37 | 100 | 28 | 15.0 | 0.41 | 16.1 | 0.44 | 0.79 | 12.4 | −69.2 | 24 | 2.27 |
| R4:U | 4.5 | −0.19 | 200 | 30 | 17.2 | 0.43 | 18.5 | 0.46 | 0.79 | 19.3 | −34.6 | 38 | 1.48 |
| R4:L | 3.8 | 0.06 | 200 | 30 | 17.2 | 0.43 | 18.5 | 0.46 | 0.79 | 12.7 | 7.3 | 25 | 0.78 |
| R5:U | 5.0 | −0.35 | 200 | 30 | 17.2 | 0.43 | 18.5 | 0.46 | 0.79 | 18.2 | −67.2 | 36 | 0.97 |
| R5:L | 4.2 | −0.12 | 200 | 30 | 17.2 | 0.43 | 18.5 | 0.46 | 0.79 | 12.9 | −21.1 | 25 | 0.80 |
| R6:U | 5.0 | −0.41 | 200 | 30 | 17.2 | 0.43 | 18.5 | 0.46 | 0.79 | 11.4 | −76.9 | 22 | 1.40 |
| R6:L | 4.3 | −0.29 | 200 | 30 | 17.2 | 0.43 | 18.5 | 0.46 | 0.79 | 8.5 | −46.9 | 17 | 1.15 |
| R7:U | 5.8 | −0.83 | 10 | 22 | 10.0 | 0.35 | 10.6 | 0.37 | 0.79 | 16.6 | −113.5 | 32 | 3.68 |
| R7:L | 5.6 | −0.64 | 10 | 22 | 10.0 | 0.35 | 10.6 | 0.37 | 0.79 | 6.8 | −86.4 | 13 | 3.29 |
| R8:U | 12.5 | −1.16 | 50 | 26 | 13.2 | 0.39 | 14.1 | 0.41 | 0.79 | 63.1 | −351.4 | 123 | 0.36 |
| R8:L | 9.0 | −0.98 | 50 | 26 | 13.2 | 0.39 | 14.1 | 0.41 | 0.79 | 26.0 | −230.8 | 51 | 2.51 |
| R9:U | 10.6 | −0.80 | 100 | 28 | 15.0 | 0.41 | 16.1 | 0.44 | 0.79 | 27.1 | −255.6 | 53 | 2.51 |
| R9:L | 11.0 | −0.55 | 100 | 28 | 15.0 | 0.41 | 16.1 | 0.44 | 0.79 | 37.3 | −201.4 | 73 | 1.57 |

[a] U ≡ upper (1220 m),
L ≡ lower (460 m).

absence of foliage significantly alters the effective thermal conductivity of a wooded area; also, the former situation may lead to larger values of $\mu$ as a result of the increased surface area, the concurrent increase in mixing, and the transfer of heat away from the canopy.

The 'developed' sites (R-3, R-4, R-5, and R-6) all have similar values of the thermal admittance, around 25 mly $s^{-1/2}$ $K^{-1}$. The difference in $\mu$ among the various building-zone types is unnoticeable; i.e., new and old residential and commercial zones all appear to be similar. One possible exception is site R-6, where $\mu$ computed from the lower level aircraft data seems somewhat low.

Site R-7 is a good check on the method since the site is simple, homogeneous, and extensive; experience dictates a low value for $\mu$ – Geiger (1965) estimates 35. The two $\mu$ values for this site are 32 and 13, averaging out to 23.

Without supporting surface observations, it is difficult to evaluate the Bo values quantitatively. Most are less than 2.5; site R-7 shows the maximum, having an average Bo of 3.5. There had been showers in the area on 8 August and hence the Bo values are not unreasonably large. It is significant that the lowest values are found for three of the four developed sites, R-4, R-5, and R-6. This is to be expected due to the increased runoff in urban and suburban areas and the corresponding decrease in evaporation.

Although the theoretical formulation used in evaluating the surface energy budget explicitly ignored energy fluxes associated with photosynthesis and anthropogenesis, the impact, if any, of such fluxes is still reflected in the measured data. Hence, in using the climatonomic theory in the evaluation of $\mu$ and Bo as residuals, we have *implicitly* accounted for the impact of such other fluxes in the determination of these parameters. For example, the particularly large Bo determined for the undeveloped sites probably reflect some impact of photosynthesis. This may explain, in part, why the largest Bo values were found for the agricultural site.

The $\mu$- and Bo-values tabulated in Table III are the result of the analysis of the first-harmonic data. Since $\mu$ and Bo are frequency-independent, all harmonics should yield similar results. Difficulties were encountered in attempting to evaluate both parameters on the basis of the second-harmonic data: $\mu$ values became negative, while Bo was often excessively large (up to 25). Several possible explanations are offered for these discrepancies: errors in the regression analysis, experimental inaccuracies, parameterization errors, and limitations in the theory – particularly in the neglect of photosynthetic and anthropogenic fluxes. Most likely, each contributes to the problem. On the assumption that the cause lay in the data, and particularly in the determination of the second-harmonic terms, a simple feedback analysis was conducted in which effective $\Delta_2 T_0$ and $\delta_2$ values were derived that forced the determination of $\mu$ and Bo values equal to the first-harmonic results. In 16 of the 18 cases, the 'effective' temperature amplitude ($\Delta_2 T_0$) differed from the original (Table III) by less than 0.7 °C; phase differences were generally larger, averaging about 0.6 rad or 70 min. Differences in both terms are certainly within the range of possible errors associated with the regression method for determining

Fourier coefficients and/or with departures from the aircraft flight track (leading to differences in scene at the nine sites from flight to flight).

## 6. Concluding Remarks

The feasibility of the climatonomical method has been demonstrated for the evaluation of differences in the surface energy budget with differences in land-use in the St. Louis area. Airborne observations of the diurnal variations in surface temperature in response to diurnal variations in available solar radiation at the surface, when combined with observations of air flow and estimates of surface roughness, enable the determination of the effective thermal admittance and Bowen ratio characteristic of the various surfaces. To achieve these results it was necessary to parameterize the atmospheric sensible heat flux appropriate to the prevailing clear summertime conditions.

More recent (August 1974) and improved airborne data over the same area are now available for analysis with an improved parameterization of the atmospheric heat flux. Since the time this analysis was completed, Lettau (1976) has proposed an alternative to the Fourier synthesis that is based on a forward integration procedure. The new procedure has the particular advantage of requiring neither a stationary nor complete diurnal data set. Analysis of the more recent data using the new procedure will be instrumental in the verification of the observed and derived surface characteristics established under this study. As a logical expansion, the same type of program could be expanded to provide a systematic evaluation of surface characteristics over a broad range of land-use types under varying meteorological conditions. In this way it will be possible to consider such interactions as the impact of soil moisture on the thermal admittance and Bowen ratio, the effect of seasonal changes in albedo, and the significance of anthropogenic sources.

## References

Changnon, S.: 1972, *1972 Operational Report for METROMEX*, Illinois State Water Survey, Urbana, Ill., U.S.A.

Geiger, R.: 1965, *The Climate Near the Ground*, 4th Ed., Harvard University Press, Cambridge, Mass., U.S.A.

Kung, E.: 1963, 'Climatology of Aerodynamic Roughness Parameter and Energy Dissipation in the Planetary Boundary Layer over the Northern Hemisphere', Section 2 of *Studies of the Effects of Variations in Boundary Conditions on the Atmospheric Boundary Layer*, Dept. of Meteorology, University of Wisconsin, Annual Report, Contract DA-36-039-AUC-00878, USAERDA, Ft. Huachuca, Ariz., U.S.A.

Lettau, H.: 1976, *Climatonomy of Arid Regions with Areas Under Irrigation*, unpublished manuscript. Dept. of Meteorology, University of Wisconsin, Madison, U.S.A.

Lettau, H. H. and Lettau, K.: 1972, *Exploring the World's Driest Climate: Scientific Results of Wisconsin Field Studies during July 1964 in the Peruvian Desert (Pampa de la Toya)*, University of Wisconsin Press, Madison, Wisc., U.S.A.

Panofsky, H. and Brier, G. N.: 1965, *Some Applications of Statistics to Meteorology*, Mineral Industries Continuing Education, Pennsylvania State College, University Park, Penn., U.S.A.

Van Wijk, W. R. (ed.): 1963, *Physics of Plant Environment*, North-Holland Publishing Company, Amsterdam, The Netherlands.